metals

MDPI

Article

Effect of Fiber-Laser Parameters on Cutting Accuracy of Thin and Thick S355JR Structural Steel Plates

Laura Cepauskaite and Regita Bendikiene *

Department of Production Engineering, Faculty of Mechanical Engineering and Design, Kaunas University of Technology, Studentu Str. 56, LT-51424 Kaunas, Lithuania; laurracep@gmail.com
* Correspondence: regita.bendikiene@ktu.lt

Abstract: Fiber lasers, the latest laser-cutting technology, are notable for their high process efficiency, cutting precision, and high cutting quality for thin materials. However, the quality of the cut significantly decreases when machining thicker materials. For now, this is a challenge for the metalworking industry. This study investigated the effects of laser power, cutting speed, and auxiliary gas pressure on the fiber-laser cutting quality of 4 and 6 mm thick S355JR steel plates. To evaluate the influence of cutting parameters on cutting quality, surface roughness, dimensional accuracy and cut taper were measured. A microscopic analysis of the laser cuts was performed, revealing the heat-affected zone, transition zone and unaffected base-material zone. Research results show that laser cutting is a complex process, and the correct choice of cutting parameters greatly influences the cutting performance and final quality. An artificial neural network was created and trained using the results from measuring the quality characteristics to achieve optimum cutting quality. The accuracy of the optimization model was assessed by control samples, which were cut using calculated optimum parameters. The actual values of the quality characteristics only slightly differ from the predicted values, showing that the optimization model is suitable for selecting cutting parameters.

Keywords: laser cutting; fiber laser; cutting quality; accuracy; process parameters; artificial neural networks

check for updates

Citation: Cepauskaite, L.; Bendikiene, R. Effect of Fiber-Laser Parameters on Cutting Accuracy of Thin and Thick S355JR Structural Steel Plates. *Metals* **2024**, *14*, 723. https://doi.org/10.3390/met14060723

Academic Editor: Umberto Prisco

Received: 15 May 2024
Revised: 8 June 2024
Accepted: 15 June 2024
Published: 18 June 2024

Copyright: © 2024 by the authors. Licensee MDPI, Basel, Switzerland. This article is an open access article distributed under the terms and conditions of the Creative Commons Attribution (CC BY) license (https://creativecommons.org/licenses/by/4.0/).

1. Introduction

Due to ever-increasing production volumes and demand, the metalworking industry is developing rapidly. The need to process different materials and their thicknesses and shapes has greatly increased, which is a big challenge for the industry. Competition in the metalworking industry is becoming increasingly fierce [1]. Recently, the metalworking industry has been looking for ways to achieve maximum process performance. This means an aspiration to produce a product as quickly as possible and at the lowest cost of materials while maintaining high quality [2]. These goals can be achieved in two ways: the intelligent utilization of available technological capabilities and trying to switch to new technological processes. So, the question arises: how can we choose one of the many methods of metal processing to meet a company's needs?

Conventional production methods are still widely used in metalworking companies, the principle of which is to remove a layer of metal as the workpiece or tool rotates. They have several advantages as they are firmly established in the manufacturing industry and have produced reliable results for many years. Since various interchangeable cutting tools are used during these technological processes, they are versatile and can be used to produce parts of complex shapes. However, they also have major drawbacks, such as being time-consuming and still requiring manual labor, and, most importantly, turning, milling, drilling, and other machining operations generate large amounts of production waste such as loose metal chips or metal shavings mixed with coolants used in machining operations [3]. Furthermore, the manufacturing sector has been identified as a significant

consumer of European electricity. Indeed, it is estimated that this sector utilizes approximately 25% [4] of all electricity generated in the continent. This observation leads to the conclusion that the manufacturing sector is also responsible for a substantial proportion of the environmental pollution released during the production of electricity [4]. As a result, there is a growing focus on sustainable manufacturing. The primary objective of this approach is to achieve the most efficient transformation of materials into final products through the use of environmentally friendly processes [5].

Consequently, to process external and internal contours quickly, non-traditional processing methods (such as abrasive water jet cutting, laser cutting, electrochemical processing, etc.) are increasingly used as an alternative to conventional recycling processes. Compared to the previously mentioned conventional machining methods, the metalworking industry is characterized by wider application possibilities and higher productivity while maintaining the same, and often even higher, machining accuracy [3,6]. These methods differ from conventional processing methods in terms of their operation principle; in particular, there is no direct contact between the tool and the cut surface during processing. The material is processed under the influence of various types of energy, such as mechanical, chemical, and thermal, which depends on the chosen cutting method. Laser cutting is mainly a thermal process in which a focused laser beam is used to melt the material at a specific location [7]. The high-power laser beam heats and fuses the material to be cut, which is pushed out from the cutting area by a coaxial gas stream, creating a gap. The operation, in general, is based on computer numerical control (CNC). The CNC controller can continuously monitor the laser-cutting head according to a pre-prepared cutting program, where the laser movement trajectory and the main cutting parameters are predicted [8]. Laser-cutting machines for cutting sheet metal typically operate within a three-axis coordinate system. The *X*-*Y* axes are parallel to the surface of the processed workpiece and define the coordinates of the movement trajectory. The *Z* axis, perpendicular to the surface of the workpiece, indicates the distance of the laser nozzle to the workpiece [9].

The popularity of laser cutting has grown rapidly mainly due to its technical capabilities, allowing industrial lasers to be used in many fields, from precision watchmaking to the aerospace industry [10]. However, although laser cutting offers new opportunities for mechanical processing, like other processes, it also has inevitable disadvantages related to the quality of the parts. During the laser-cutting process, high surface roughness, insufficient accuracy of dimensions and cut geometry, slag or temperature-affected zones are encountered.

Laser cutting is usually followed by other technological processes (e.g., forming, joining, coating). For this reason, the quality of the part's laser processing is of the utmost importance, as surface defects can affect other operations and the accuracy and quality of the final product. As an example, during welding, an uneven cutting edge can make it difficult to position the part correctly, and the dimensional accuracy of the welded assembly can also decrease. Moreover, the quality of the cutting edges is also crucial during the final technological operations, such as powder-coating or galvanizing. The adhesion of the coating is directly dependent on the quality of the cutting edges, as evidenced by research studies [11,12]. Solving such laser-cutting quality problems is particularly important because the insufficient quality of manufactured parts can affect their durability and reliability [13].

For this reason, scientists conduct various studies to determine the causes of quality defects in laser-processed parts [14]. The main research direction is the evaluation of the influence of laser-cutting input parameters (cutting speed, laser power, type of auxiliary gas, laser beam pressure or focal length) on the quality of processed components and the search for the best parameter sets [15]. However, it should be noted that the selection of parameters often becomes difficult when changing the cutting parameters, which improves the values of some quality characteristics but simultaneously worsens other characteristics. However, the selection of these parameters is often conducted through a trial-and-error approach, which is an ineffective method that may result only in increased operator time

and material costs and ultimately may not achieve the optimal cutting quality [14]. To avoid this, it is very effective to perform optimization, during which the values of the input parameters can be found with which the cutting quality would be optimal, i.e., all evaluated characteristics should meet at least the minimum requirements. For some time, analytical, numerical and experimental techniques were employed to investigate the laser-cutting process [16,17]. However, conventional optimization methods are often ineffective in improving the laser-cutting process due to the multitude of factors influencing the process. To fully identify and resolve quality issues and optimize the process, it is essential to conduct extensive research [17]. Recently, to reduce the number of experimental trials, more advanced methods based on artificial intelligence (AI) have been used, which, even with limited data, are capable of identifying complex relationships between variables [17]. It follows that artificial intelligence can be practically applied to the resolution of engineering problems, the monitoring of production processes, and the automatic correction of process parameters in the event of deviations beyond the established tolerance limits. Recent advancements in the field of AI have enabled the application of these techniques to the modelling and optimization of the laser-cutting process [16]. For example, Ref. [18] used ANNs to forecast surface roughness and cutting region temperature in relation to laser power, sheet thickness, and auxiliary gas pressure when processing Al6061T6 alloy. Results shows that a mean error value between predicted and experimental values was 0.66% for the cutting region temperature and 5.79% for the surface roughness [18]. The creation of ANNs enabled a more comprehensive understanding of the relationships between surface roughness and cutting region temperature, as influenced by each of the parameters under investigation. In conclusion, the advancement of manufacturing processes can only be achieved through the implementation of advanced solutions such as the Internet of Things (IoT), machine learning, and artificial intelligence [19,20]. These methods, acting in synergy, can collect data on the quality characteristics of the laser-cutting process and, when deviations are observed, control the process parameters to bring the quality back to optimum [21,22].

Currently, the integration of such advanced tools into a real production environment is unfortunately still a challenging process because when creating optimization models, first, there is a need to know the influence of each process parameter on the product quality, and secondly, there is a need to understand the essence of the process perfectly. In the metalworking sector, several types of laser-cutting machines (such as CO_2 or fiber) are used, which differ in their principle of operation. Such a difference causes difficulties in the analysis of the quality characteristics of laser cutting since quality characteristics studies must be carried out separately for each type of laser. Since the first industrial use of laser cutting in 1967, when researchers tried to process a 1 mm thick steel plate with a 300 W CO_2 type laser [23,24], there have been obvious advances in laser processing—lasers are much more powerful, and more types of lasers are used in the manufacturing industry, which are classified according to the active medium where the laser beam is generated. The active material of the CO_2-type laser is a mixture of carbon dioxide (CO_2), nitrogen (N_2) and helium (He) gases, and the fiber-type laser is an optical fiber. CO_2 lasers have been used for cutting for a long time, but recently, the newer fiber-laser technology has become increasingly popular. The main characteristics that distinguish CO_2 and fiber lasers are wavelength (10.6 μm and 1.07 μm, respectively), energy efficiency (5–8% and 20–30%), maintenance (every 2000 h and every 10,000 h) and device area occupied (large and small) [23]. It is important to mention that the laser's wavelength greatly influences the efficiency of the process. A beam with a shorter wavelength is more easily absorbed by the material being cut, so fiber lasers, due to their ten-times shorter wavelength, have a higher cutting efficiency, acceleration, and maximum cutting speed [8,25]. In addition, the shorter wavelength of the fiber laser can cut various materials, such as copper, nickel and its alloys or composite materials [23]. Among the advantages of fiber lasers, infrequent servicing can also be attributed to a reduction in service costs and device downtime. The advantages of the mentioned "fiber"-type lasers can be attributed to rare maintenance, which reduces

service costs and device downtime. It has been established that fiber lasers can be a good alternative to other plate-metal processing technologies, such as coordinate stamping or guillotine cutting. It is often even superior because the high speed of cutting thin-plate metal creates less residual stress in the material than mechanical cutting. In addition, the laser can cut a variety of contours without the additional tools required to cut the contour using coordinate stamping [25].

On the other hand, the main disadvantages of fiber lasers are their high cost and the deterioration of cutting quality when processing thicker materials [23]. It is important to mention that when the thickness of the material exceeds 4 mm, the quality of the processing significantly decrease [24,26]. Consequently, in order to utilize this type of laser for processing such materials, it is essential to pay close attention to the cutting process with regard to the input parameters. Therefore, the main goal of this scientific article is to evaluate the influence of laser-cutting input parameters when cutting plates thicker than 4 mm and to find an optimal set of input parameters. A detailed review of the published sources showed that much less research had been conducted on fiber lasers than on CO_2 lasers. Further research is needed on the cutting quality of the first-type lasers. Considering this, it was decided in this research study to evaluate the influence of fiber-laser cutting input parameters when cutting plates thicker than 4 mm. The quality of the cut was the primary area where these parameters have a significant impact. Consequently, the primary objectives of the research were to measure the roughness of the cut surface, evaluate the accuracy of laser cutting, determine the kerf taper, evaluate the laser-cutting thermal effect for the material, and finally, create a laser-cutting quality optimization model based on artificial neural networks (ANNs).

2. Materials and Methods

Hot-rolled mild S355JR steel (EN 1.0045) specimens with thickness of 4 and 6 mm were used for laser-cutting experiments. This unalloyed structural steel can be used to produce parts that will be subjected to various loads due to its chemical composition and mechanical properties (Table 1). Furthermore, S355JR steel has good weldability, allowing for a wide range of welding methods [27]. Due to its widespread use in the metalworking industry, it was selected for further research.

Table 1. Characteristics of S355JR steel [27,28].

Steel	**Chemical Elements, Mass %**					
	C	Mn	P	S	Si	Fe
S355JR	≤0.23	≤1.6	≤0.05	≤0.05	≤0.05	≥98.02
	Mechanical Properties					
	Tensile strength σ_u, MPa	Yield strength σ_y, MPa	Hardness, HB	Density, kg/m^3		
	470–630	355	146–187	7850		

Laser-cutting quality tests were performed using a 4 kW Prima Power Platino Fiber 1530 fiber-laser cutting machine(MASZYNERIA SP. Z O.O., Jelenia Góra, Poland).

A number of factors can significantly influence the quality of laser cutting, including laser power, cutting speed, auxiliary gas pressure, focal plane position (FPP), laser stand-off distance, and laser nozzle type and diameter. Despite the considerable influence that all these factors have on cutting, the present study focuses on examining the effects of laser power, cutting speed, and auxiliary gas pressure.

During the cutting experiments, these key process parameters were varied, while the values of the stand-off distance (1.2 mm), focal plane position (8 mm), and frequency (1000 Hz) remained constant. The laser-cutting process for both material thicknesses was performed using oxygen auxiliary gas and a conical copper laser nozzle of Ø1.5 mm diameter.

The choice of cutting parameters has a direct effect on the amount of linear energy transferred to the cutting zone. Linear energy is calculated according to Equation (1) [29]:

$$E_l = \frac{P \times t}{L}, \tag{1}$$

where E_l—linear energy, J/mm; P—laser power, W; t—machining time, s; L—laser-cutting length, mm.

The machining time t is calculated:

$$t = \frac{60 \times L}{v}, \tag{2}$$

where v—cutting speed, mm/min.

Inserting Equation (2) into Equation (1) gives a simplified Equation (3) for calculating linear energy:

$$E_l = \frac{60 \times P}{v}. \tag{3}$$

The quality characteristics of the samples, such as surface roughness, cutting accuracy, kerf taper and heat-affected zone depth were measured to evaluate the influence of the laser-cutting parameters on the cut quality. First, the roughness of the side-cut surface of the samples cut with different parameters was determined using a Mitutoyo SJ-210 profilometer (Kawasaki, Japan). According to ISO 4287:1997 [30], a measuring speed of 0.5 mm/s was chosen, and the measuring distance was l_n = 12.5 mm, divided into five equal sampling lengths of l_r = 2.5 mm each. The following roughness parameters were selected for the roughness measurement of laser-cut samples: average surface roughness *R*a, the average roughness depth *R*z, and the maximum roughness depth *R*z1max [30]. The surface roughness of each sample was evaluated in the middle of its thickness. Also, measurements were performed twice, once on the longer side and once on the shorter side, and then the average roughness parameters (*R*a, *R*z and *R*z1max) were calculated for each sample.

The quality of laser cutting can also be assessed by analyzing dimensional accuracy. For this purpose, the 15 dimensions of the sample shown in Figure 1 were chosen. For measuring the defined dimensions, a Mitutoyo CRYSTA-Apex 9106 (Kawasaki, Japan) coordinate-measuring machine with a measuring accuracy of 0.002 µm was used. The measurements were carried out in the laboratory at a constant temperature of 20 °C.

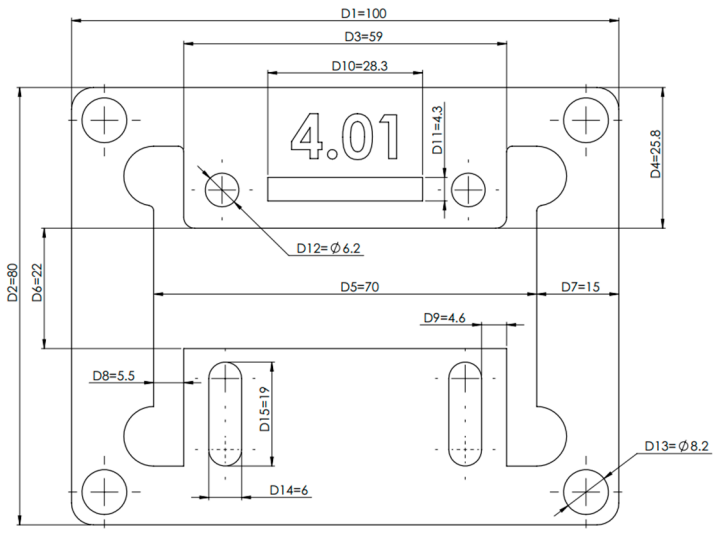

Figure 1. Sketch of the sample (dimensions in mm).

The dimensional deviation was calculated by comparing the measured dimension values with the nominal dimensions determined before cutting. The obtained cutting accuracy was compared with the dimensional tolerances specified in ISO 9013:2017 [31] for parts produced by thermal cutting methods such as laser or plasma cutting. Since the laser cut is often not perpendicular, the selected dimensions were measured on the top and bottom surfaces of the sample. From these measurements, a kerf taper was calculated, which describes the difference in each measured dimension on both surfaces of the sample. The kerf taper angle was calculated using Equation (4) [32]:

$$\alpha = \left(\frac{TS - BS}{2 \cdot t}\right) \times \frac{180}{\pi}, \tag{4}$$

where α—kerf taper angle, °; TS—dimension value on the top surface, mm; BS—dimension value on the bottom surface, mm; t—thickness of the sample, mm. Based on the kerf taper angle value, the direction of the taper can be determined. A positive angle indicates that the cut tapers from the top to the bottom surface, while a negative angle indicates that the cut tapers from the bottom to the top surface.

In addition, to analyze the thermal effect of laser cutting on the metal alloy, six samples were selected for further analysis. The selection was based on the results of previous experiments on surface roughness, dimensional and geometric accuracy. Samples characterized by good, medium, and poor cutting quality were selected for further analysis. To evaluate the thermal impact on the metal alloy, smaller test pieces were taken from the selected samples and molded into epoxy resin. A LAM PLAN SMARTLAM 2.0 grinding machine was used to grind and polish the test pieces. Grinding was performed in four stages using different types of sandpaper (180, 600, 1500 and 2500) and by changing the grinding direction after each stage. Following this, a diamond emulsion was used to polish the surface to a mirror-like finish. After polishing, the surface of the test pieces was etched with Nital (3% nitric acid (HNO_3)). The heat-affected zone (HAZ) was analyzed, and microstructure images were observed using a Zeiss AXIO Scope. A1 microscope (Oberkochen, Germany). Finally, quality characteristics measurements of samples collected during the laser-cutting quality experiments were analyzed using artificial neural networks (ANNs) based on artificial intelligence (AI). This method was selected because conventional optimization methods are often ineffective in improving the laser-cutting process due to the multitude of factors influencing the process. To fully identify and resolve quality issues and optimize the process, it is essential to conduct extensive research. However, to reduce the number of experimental trials, more advanced methods based on artificial intelligence (AI) are used, which, even with limited data, are capable of identifying complex relationships between process input, process parameters, and output parameters—quality characteristics [17]. This method simulates the neural network of the human brain for solving complex nonlinear problems. Thus, the data set containing the quality characteristics of the samples was transformed into an artificial neural network structure. The ANN has two main layers of neurons: an input layer, which defines the input variables, and the output layer, which defines the target values of the output parameters. Also, ANNs have hidden layers of neurons. The number of hidden layers depends on the complexity of the problem being solved [16]. According to the algorithm shown [17], the feed-forward ANN was designed using Matlab's Neural Network Toolbox software (2017b (11.0)) add-on. Process optimization was performed to determine the appropriate laser-cutting parameters, including laser power, cutting speed, and auxiliary gas pressure, to achieve an optimal quality of laser-cut parts. The developed ANN was used to calculate the value of the objective function that should be minimized. This optimization model based on AI was applied to optimize the quality characteristics of both 4 and 6 mm thickness analysis. According to the laser-cutting parameter sets calculated during the optimization, control samples were cut, and the quality characteristics of these specimens were measured. The results were compared with the values predicted by the ANN, and the accuracy of the optimization model was evaluated.

3. Results and Discussion

To study the influence of the main laser-cutting parameters (laser power, cutting speed, oxygen auxiliary gas pressure) on the cutting quality, 24 cutting tests were performed on 4 and 6 mm thick mild steel plates. The selected values of the cutting parameters are listed in Tables 2 and 3. One sample was cut using each set of parameters.

Table 2. Cutting parameters of 4 mm thick specimens.

Cutting Test	Laser Power, kW	Cutting Speed, mm/min	Auxiliary Gas Pressure, Bar	Linear Energy, J/mm
4.01	3.8	3500	0.55	65.14
4.02	4.0			68.57
4.03	3.2			54.86
4.04	2.8			48.00
4.05	3.8	3200	0.55	71.25
4.06		4000		57.00
4.07		4500		50.67
4.08		2900		78.62
4.09		3500	0.30	65.14
4.10 *			0.15	
4.11			1.00	
4.12			1.50	

* Unsuccessful cutting.

Table 3. Cutting parameters of 6 mm thick specimens.

Cutting Test	Laser Power, kW	Cutting Speed, mm/min	Auxiliary Gas Pressure, Bar	Linear Energy, J/mm
6.01	4.0	2900	0.60	82.76
6.02	3.5			72.41
6.03	3.0			62.07
6.04 *	2.0			41.38
6.05	4.0	3300		72.73
6.06 *		3700		64.86
6.07		3500		68.57
6.08		2400		100.00
6.09		2900	2.00	82.76
6.10			3.00	
6.11			4.00	
6.12			1.50	

* Unsuccessful cutting.

The data in Table 2 show that the 4 mm thick samples were not cut in cutting test 4.10, although the linear cutting energy (65.14 J/mm), compared to other cutting tests, was sufficient to melt the material. However, the pressure of the auxiliary gas was too low to remove the molten material from the cut zone properly. Analyzing the 6 mm thick cutting test results in Table 3, it is evident that when the laser power was reduced to 2 kW, the linear energy applied to the cutting zone was reduced to 41.38 J/mm.

As a result, sample 6.04 was not cut properly due to insufficient linear energy. Also, sample 6.06 was not cut when the cutting speed was increased to 3700 mm/min, but in this case, the linear energy was 64.86 J/mm. On the other hand, it can be observed that in the cutting test of the 6.03 sample, when the energy was lower (62.07 J/mm), the sample was successfully cut. Therefore, it can be concluded that although the linear energy obtained during the cutting process is sufficient, increasing the cutting speed has a greater influence on the proper removal of material from the cutting zone than the laser power. Similar findings regarding the unsuccessful laser-cutting process when increasing the cutting speed

were observed in another research study [33]. In this study, the effect of varying laser-cutting speeds on the machining of stainless- and carbon-steel plates with thicknesses ranging from 30 to 110 mm was investigated. When the cutting speed was too high, the sample was not cut properly.

3.1. Results of the Surface Roughness Measurements

To analyze the influence of the laser-cutting parameters on the roughness of the cut surface, the surface roughness characteristics (*R*a, *R*z and *R*z1max) of 21 samples were measured (the surface roughness of the uncut specimens was not measured). The obtained data of the roughness parameters were analyzed to evaluate their dependence on the laser-cutting parameters used for each specimen cutting. It was found that the parameters of the cutting process significantly affected the surface roughness of the 4 mm thick specimens. The curves in Figure 2 show that the cutting test with the lowest average surface roughness *R*a (1.264 µm) was 4.09.

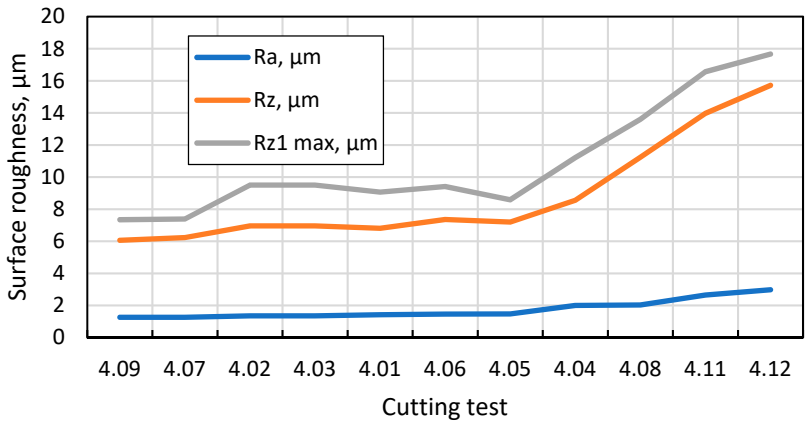

Figure 2. Variation of surface roughness of 4 mm thick samples.

This test was performed with laser power of 3.8 kW, cutting speed of 3500 mm/min and auxiliary gas pressure of 0.3 bar. In cutting test 4.12, when the cutting power was 3.8 kW, the cutting speed was 3500 mm/min, and the auxiliary gas pressure was increased to 1.5 bar, the maximum average surface roughness was measured (2.979 µm). Analyzing the dependence curves of cut surface roughness characteristics and the cutting parameters shown in Figure 3, it can be observed that the average surface roughness Ra, as opposed to *R*z and *R*z1max, shows only a small variation. However, it is observed that by increasing laser power and cutting speed, lower surface roughness can be achieved.

However, the opposite trend of roughness variation can be observed when analyzing the influence of auxiliary gas pressure while keeping other cutting parameters constant (P = 3.8 kW, v = 3500 mm/min). The lowest values of surface roughness were observed when the auxiliary gas pressure was 0.3 bar, and the roughness increased with increasing auxiliary gas pressure.

To evaluate the effect of thickness on the roughness of the cut surface, 6 mm thick samples were also measured. The results of the surface roughness measurements are shown in Figure 4. The curves depict that specimen 6.07 had the lowest average surface roughness *R*a (1.116 µm) when the laser power was set to 4.0 kW, the cutting speed was 3500 mm/min, and the auxiliary gas pressure was 0.6 bar. Conversely, sample 6.11 (P = 4.0 kW, v = 2900 mm/min, p = 4.0 bar) had the highest average surface roughness (5.241 µm).

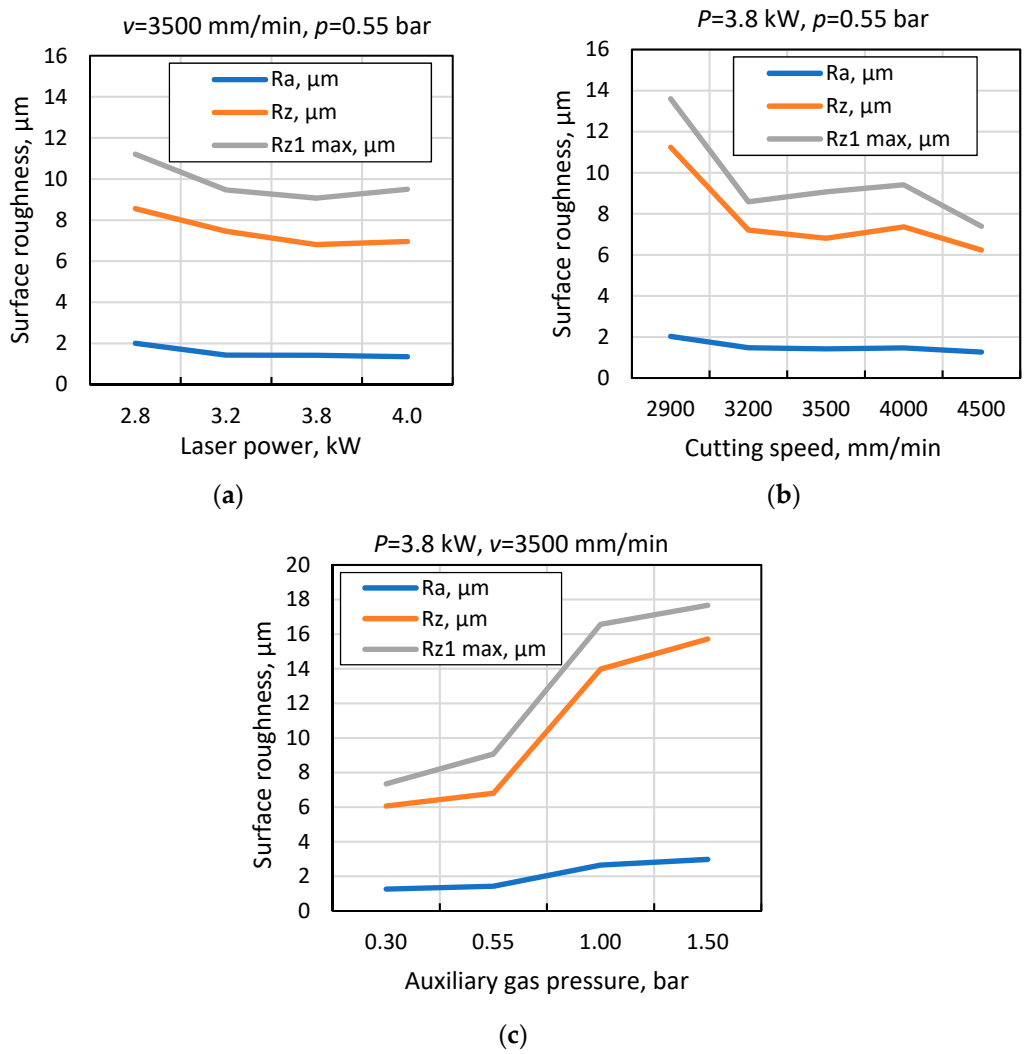

Figure 3. Variation of surface roughness of 4 mm samples under the influence of cutting parameters: (**a**) Laser power *P*; (**b**) Cutting speed *v*; (**c**) Auxiliary gas pressure *p*.

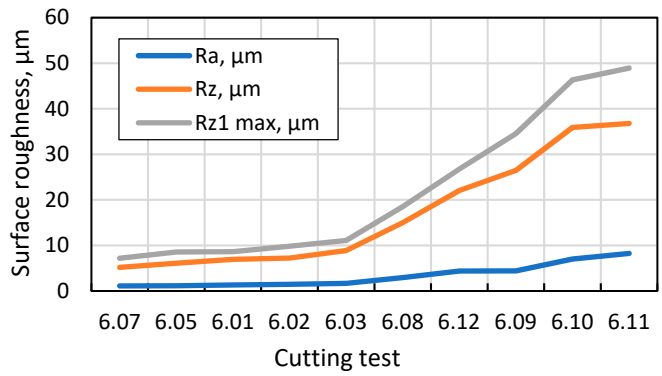

Figure 4. Variation of surface roughness of 6 mm thick samples.

Analyzing the curves depicting the dependence of the surface roughness characteristics of 6 mm thick samples on the cutting parameters (Figure 5), the same tendency was observed as in the case of the discussed 4 mm thick samples.

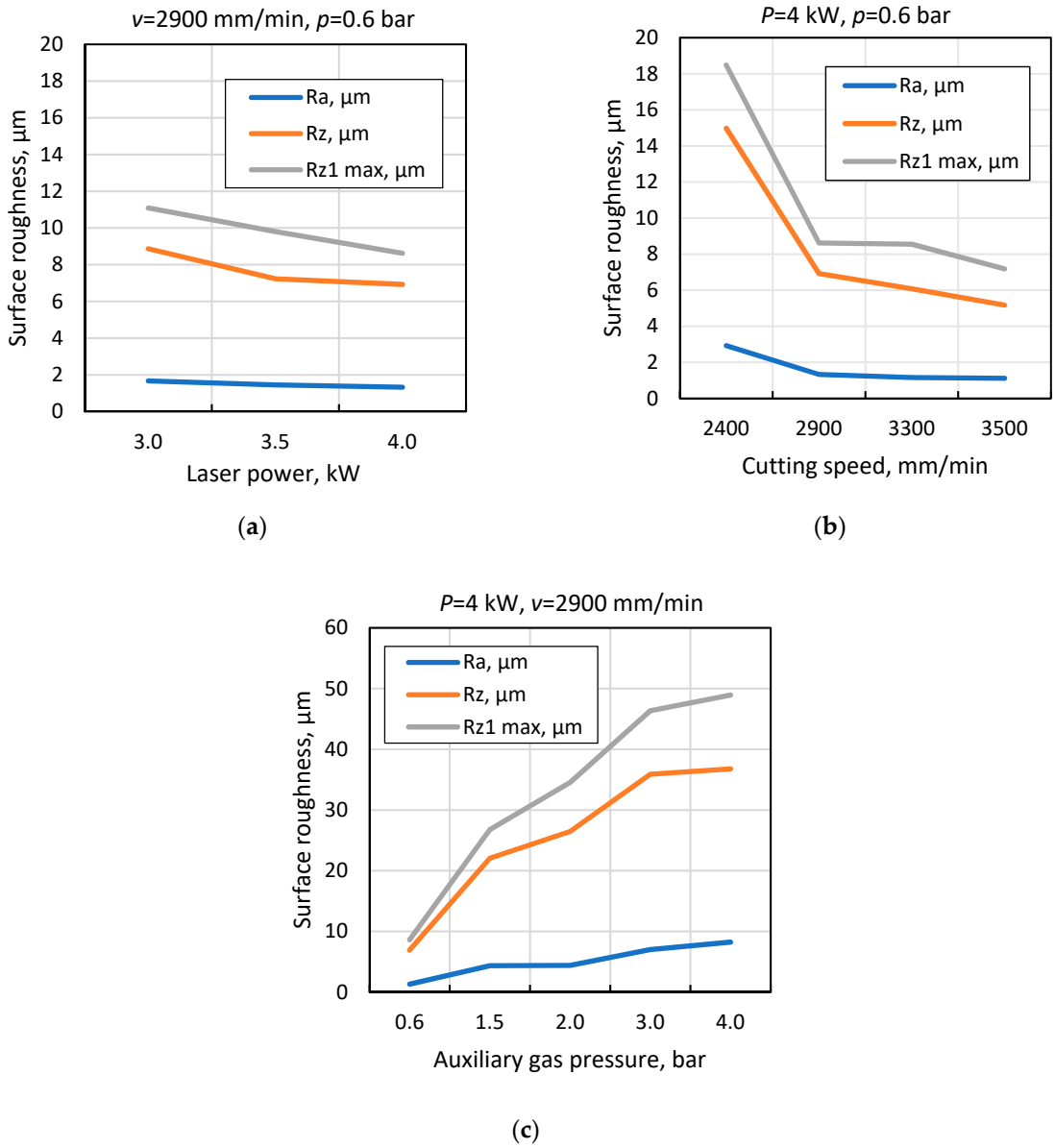

Figure 5. Variation of surface roughness of 6 mm samples under the influence of cutting parameters: (**a**) Laser power *P*; (**b**) Cutting speed *v*; (**c**) Auxiliary gas pressure *p*.

However, comparing cuts of different thicknesses with almost the same cutting parameters (P = 4 kW, v = 3500 mm/min, p = 0.55–0.6 bar), the average surface roughness *R*a of 6 mm thick sample 6.07 is equal to 1.116 µm, lower than the surface roughness of sample 4.02 (1.353 µm). Therefore, it can be assumed that as the material thickness increases, the roughness of the cut surface decreases. The results of the research on the roughness of the cut surface confirm the results of the experiments conducted by other scientists. For instance, comparing the roughness measurements of the cut surface of the analyzed 4 and 6 mm thick samples with those of another study [15], which used a 2 mm thick plate cut with a fiber laser, it can be concluded that regardless of the thickness of the material, the roughness of the cut surface increases when the laser power and cutting speed are reduced. The surface roughness is also strongly affected by the pressure of the auxiliary gas. The surface roughness will increase significantly if the pressure is too high.

3.2. Results of Cutting Accuracy Assessment

To investigate the effect of different laser-cutting parameters on the accuracy of the laser-cutting process, 15 dimensions of the lower and upper surfaces of each sample were measured, and the deviations of these dimensions from the nominal dimensions were calculated. Analyzing the curves in Figure 6, which show the relationship between the dimensional deviation of 4 mm thick samples and the selected laser-cutting parameters, it can be seen that only the laser power has a significant effect on the accuracy of laser cutting.

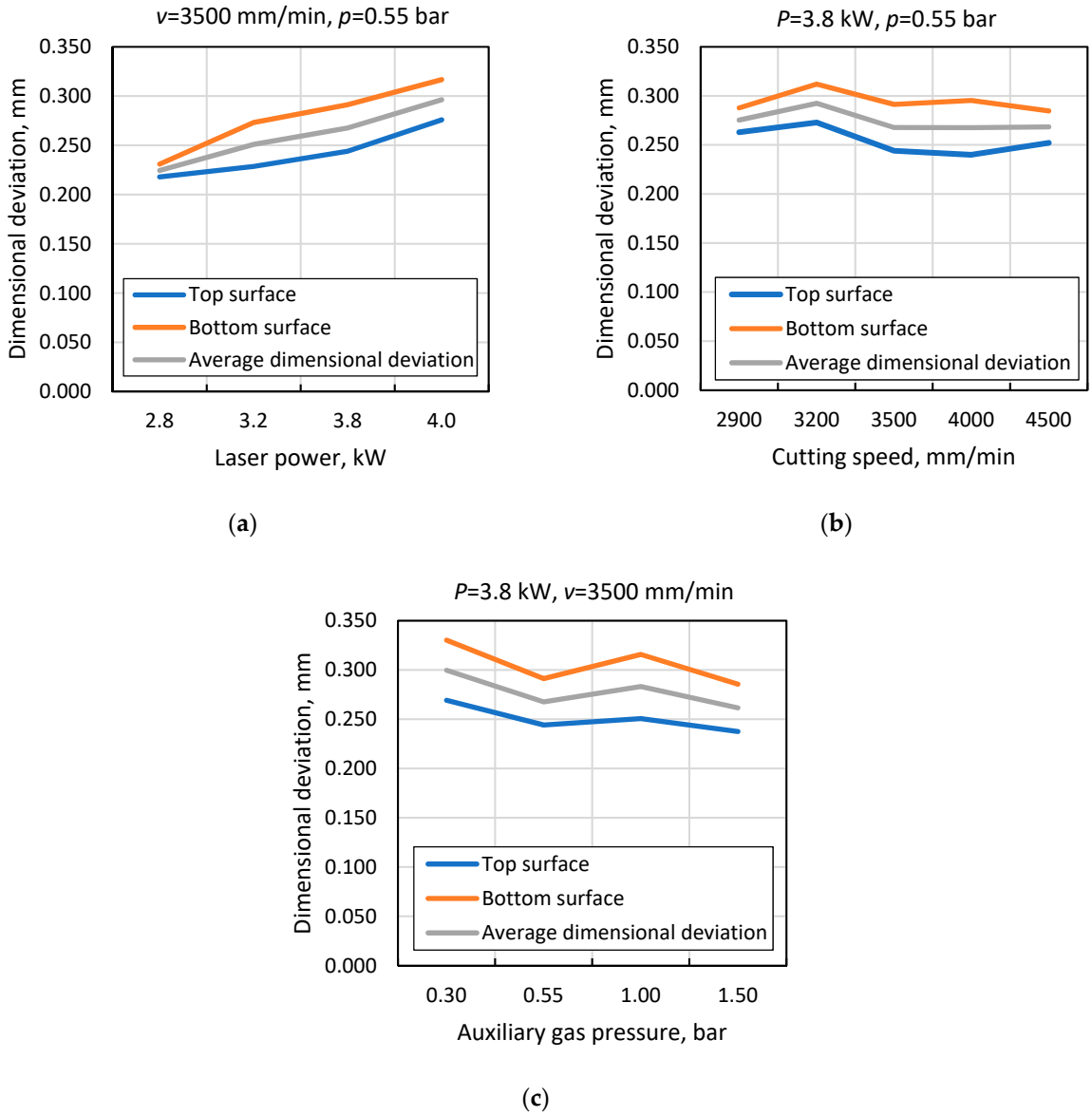

Figure 6. Variation of dimensional deviation of 4 mm samples as a function of cutting parameters: (**a**) Laser power P; (**b**) Cutting speed v; (**c**) Auxiliary gas pressure p.

As the power increases, the deviation of the sample's dimensions from the nominal dimensions also increases, resulting in lower cutting accuracy. The reason for this may be that using a higher-power laser beam for cutting makes the material melt more easily, resulting in more material being removed from the cut area. Also, increasing the cutting speed or the auxiliary gas pressure does not significantly affect the dimensional accuracy.

When evaluating the influence of cutting parameters on the cutting accuracy of 6 mm thick samples (Figure 7), the same effect of increasing laser power on cutting accuracy (as seen for 4 mm thick samples) is observed. However, in this case, a more significant

influence of the auxiliary gas can be seen—as the auxiliary gas pressure increases, the cutting accuracy decreases. It is important to mention that the cutting of the 6 mm thick samples by increasing the auxiliary gas pressure was performed at a wider range of values of this parameter (from 0.6 bar to 4 bar) than the discussed 4 mm thick tests, where the auxiliary gas pressure was only increased to 1.5 bar. The dimensional deviation increases significantly when the pressure is increased to 4 bar, so it can be assumed that during such a cutting process, due to the high gas pressure, higher vibrations occur in the device, which reduces the cutting accuracy.

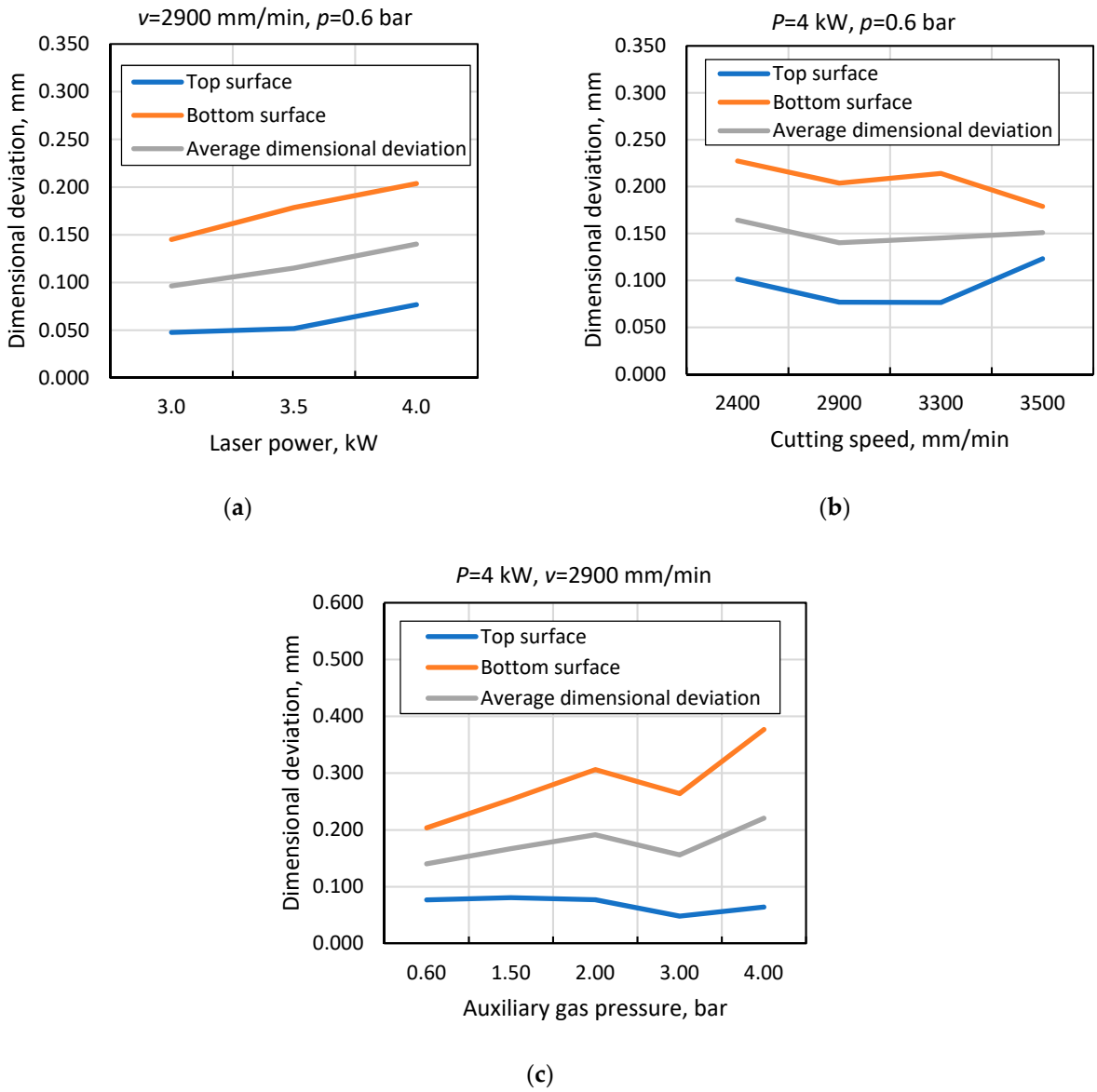

Figure 7. Dimensional deviation variation of 6 mm samples as a function of cutting parameters: (**a**) Laser power P; (**b**) Cutting speed v; (**c**) Auxiliary gas pressure p.

Figure 8 shows that the highest cutting accuracy for a 4 mm thick plate was achieved in test 4.04 (P = 2.8 kW, v = 3500 mm/min, p = 0.5 bar). The average deviation of the sample dimensions from the nominal values was equal to 0.225 mm. However, the dimensional tolerance for laser cutting of 4 and 6 mm thick plates, according to ISO 9013:2017, is ±0.2 or ±0.25 mm, depending on the dimension being measured. Therefore, the accuracy of sample 4.04 only partially meets the requirements (five measured dimensional values are outside the tolerance limits). In contrast, the sample cut in test 4.09 had the lowest accuracy (average

dimensional deviation equal to 0.3 mm) when the laser power was equal to 3.8 kW, the cutting speed was equal to 3500 mm/min, and the auxiliary gas pressure was equal to 0.3 bar.

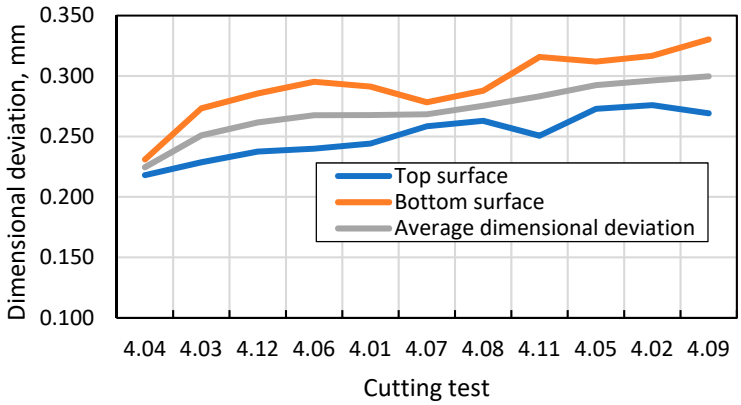

Figure 8. Dimensional deviation variation of 4 mm thick samples.

Significantly higher dimensional accuracy was observed when analyzing the accuracy values obtained from the 6 mm thick samples (Figure 9). For instance, sample 6.03 (P = 3.0 kW, v = 2900 mm/min, p = 0.6 bar) had the smallest average dimensional deviation, equal to 0.096 mm. All dimensional measurements for this sample are within the tolerance limits. For the remaining 6 mm thick samples, the average dimensional deviation increases to 0.221 mm. This maximum value was measured at a laser power of 4.0 kW, a cutting speed of 2900 mm/min, and an auxiliary gas pressure of 4 bar during cutting test 6.11. It is important to note that all the measured dimensions of the top surface of this sample are within the tolerance limits (the deviation of the top surface is equal to 0.073 mm), but extremely poor accuracy is observed on the bottom surface of the sample (0.368 mm). It can be assumed that due to the high pressure of the auxiliary gas, the molten material was more easily removed from the cutting area, resulting in a wider cut kerf. Furthermore, when comparing the dimensional accuracy on different surfaces of the samples of both thicknesses studied, it was also noticed that the dimensional accuracy is higher on the top surface.

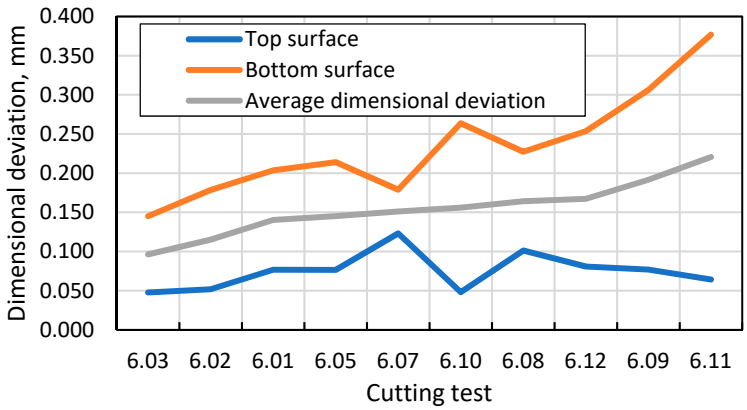

Figure 9. Dimensional deviation variation of 6 mm thick samples.

The results of the dimensional accuracy of 6 mm thick samples can be compared to similar research [23]. In this study, the authors compared the cutting accuracy of CO_2 and fiber lasers when machining 6 mm thick S235JR steel. The cutting tests were performed with a linear energy of 55.4 J/mm. The linear energy value chosen by the authors is closest to the linear energy of specimen 6.03, which was 62.07 J/mm. The average dimensional deviation of this sample was 0.096 mm, which is greater than the dimensional deviation (0.066 mm) found during the authors' fiber-laser study. However, as previously mentioned, this 6 mm thick sample was the most accurate, so it can be assumed that the lower linear energy leads to higher dimensional accuracy [23]. When assessing the effect of material

thickness on dimensional accuracy, the obtained results can be compared with another study [34]. In this paper, the kerf width of AISI 304 stainless steel samples cut by CO_2 and fiber lasers with thicknesses ranging from 1 to 10 mm were measured. Analysis of the results showed that an increase in material thickness resulted in a wider kerf and lower dimensional accuracy [34]. Conversely, the results for the 4 and 6 mm thick S355 steel samples were opposite, with the 6 mm samples being more accurate. This suggests that the material selection can have a significant effect on dimensional accuracy.

3.3. Results of the Kerf Taper Evaluation

The kerf taper was estimated using the measurement results of samples on different surfaces. This quality characteristic was determined by subtracting the value of the same dimension on the bottom surface from the dimension on the top surface. After evaluating the dependence curves of the kerf taper of the 4 mm thick specimens on the cutting parameters shown in Figure 10, it can be observed that the choice of the cutting parameters also affects the cut geometry.

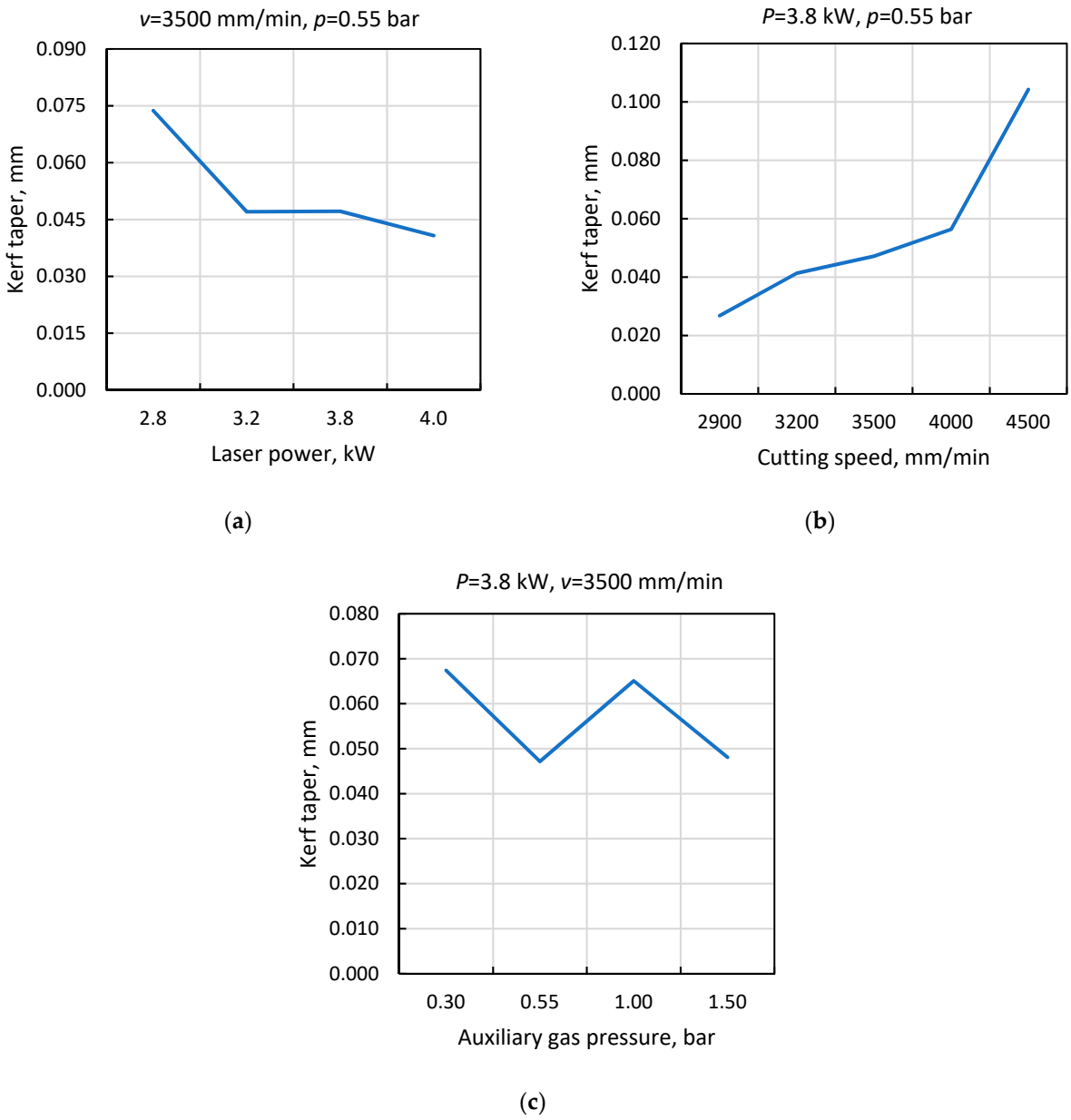

Figure 10. Variation of the kerf taper of 4 mm samples as a function of cutting parameters: (**a**) Laser power *P*; (**b**) Cutting speed *v*; (**c**) Auxiliary gas pressure *p*.

For instance, increasing the laser power reduces the kerf taper. Also, a lower cutting speed leads to a straighter cut shape. Conversely, increasing the auxiliary gas pressure from 0.3 bar to 1.5 bar does not significantly change the cut shape.

The curves in Figure 11 show the relationship between the accuracy of the cutting geometry and the cutting parameters of the 6 mm thick samples and show the same tendency of the kerf taper variation as for the 4 mm thick samples. However, it is noticeable that increasing the auxiliary gas pressure over a wider range of values increases the taper of the cut. Therefore, it can be concluded that only a significant increase in pressure can affect the shape of the cut.

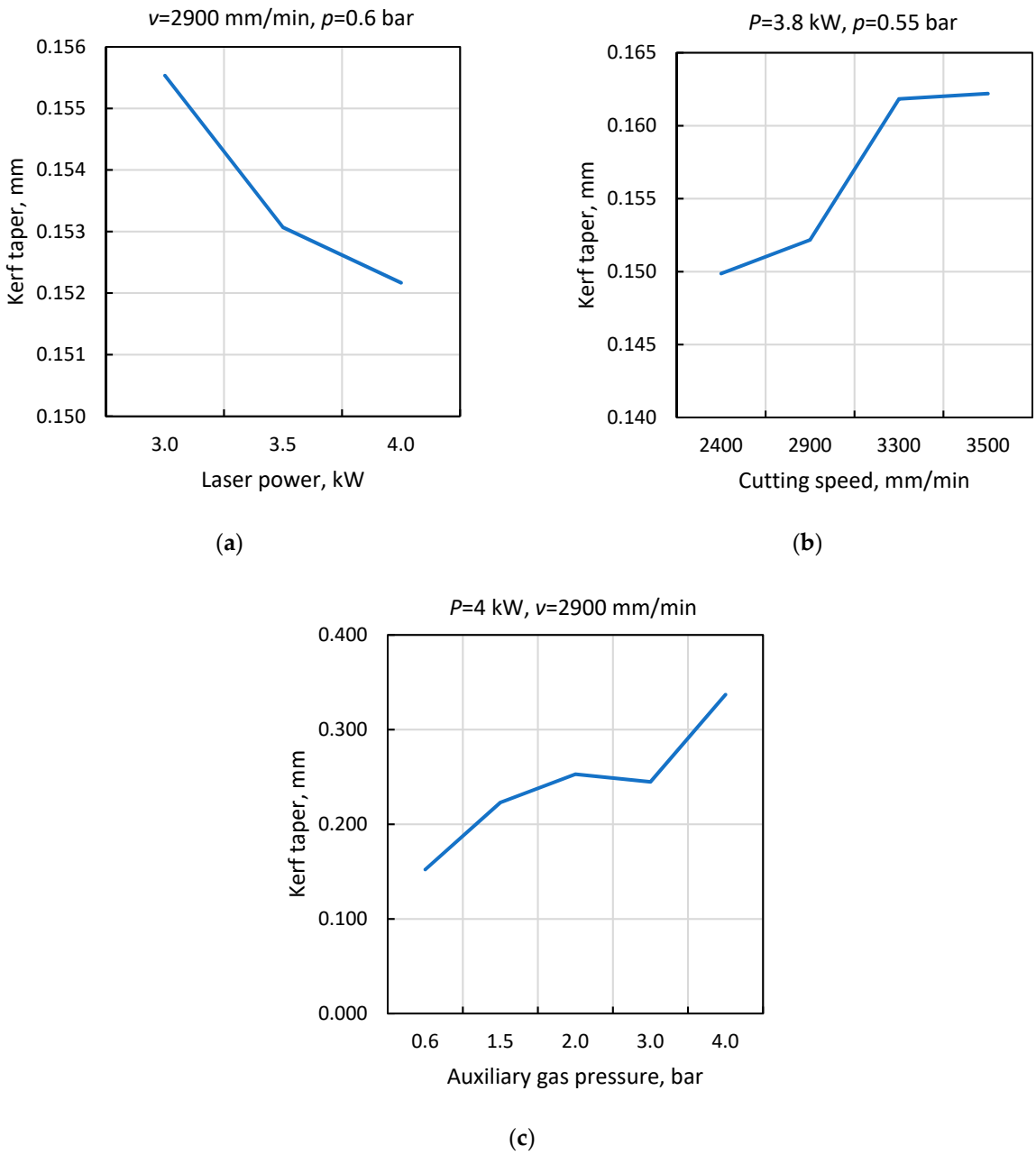

Figure 11. Variation of kerf taper of 6 mm samples as a function of cutting parameters: (**a**) Laser power *P*; (**b**) Cutting speed *v*; (**c**) Auxiliary gas pressure *p*.

The smallest kerf taper (0.027 mm) and kerf taper angle (0.192°) were achieved during cutting test 4.08, when the laser power was equal to 3.8 kW, the cutting speed was 2900 mm/min, and the auxiliary oxygen gas pressure was 0.55 bar (Figure 12). On the

other hand, the most irregular cut was obtained when cutting sample 4.07 (P = 3.8 kW, v = 4500 mm/min, p = 0.55). The kerf taper of this specimen is 0.104 mm, and the kerf taper angle is 0.747°. Comparing the cutting parameters of these two samples, it is noticed that the only difference is the cutting speed, which, when increased, resulted in an irregular cut geometry.

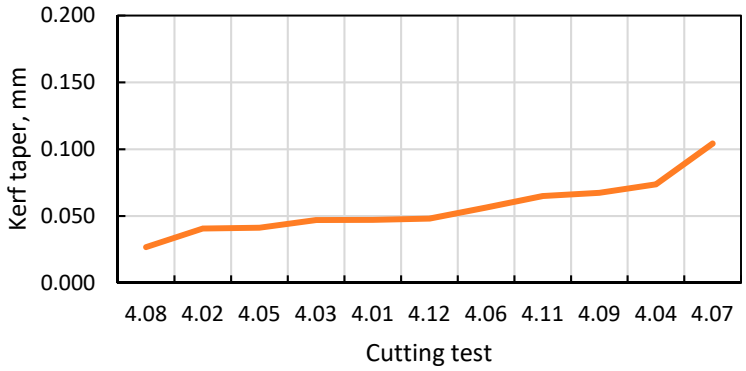

Figure 12. Variation of kerf taper of 4 mm thick samples.

Also, the curves depicted in Figure 13 show the variation of the kerf taper angle of the 6 mm thick samples. The most accurate cut geometry was achieved in test 6.08 (P = 4.0 kW, v = 2400 mm/min, p = 0.6 bar) with a kerf taper of 0.15 mm and a kerf taper angle of 0.716°. Samples 6.09–6.12, where the auxiliary gas pressure was increased during cutting, showed the worst and the highest kerf taper cutting results. Therefore, it is not recommended to use a high pressure of auxiliary gas during cutting to achieve a straighter cut geometry. Comparing the accuracy of the cutting geometry of analyzed samples of different thicknesses, it is obvious that the accuracy of the cutting geometry decreases with the increase in the thickness of the processed material.

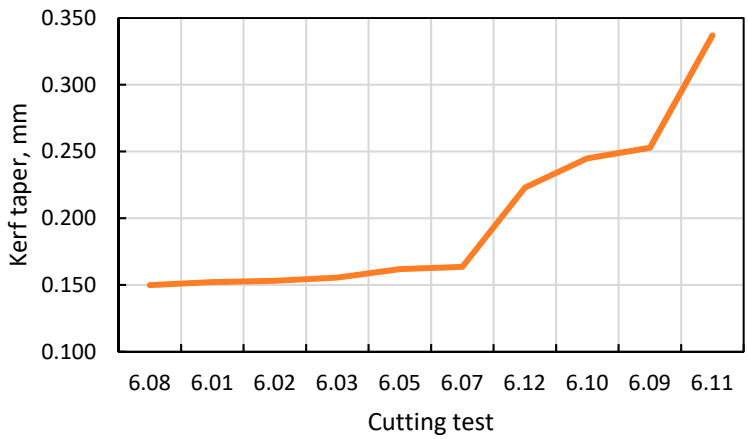

Figure 13. Variation of kerf taper of 6 mm thick samples.

Comparing the results with other studies, the widening of the cut toward the bottom of the sample is unusual in laser-cutting studies. However, it should be noted that the type of laser used for cutting has the greatest influence on the shape of the cut. In their study, authors [34] compared the cut geometry of AISI 304 stainless steel samples treated with CO_2 and fiber lasers and observed that the cut narrowing toward the bottom is typical for CO_2 lasers. These results can be confirmed by another study [35] in which samples of aluminum $AlMg_3$, steel S235JR and stainless steel AISI 304 were treated with a CO_2 laser. The choice of material did not affect the shape of the cut. In all cases, a narrower cut was observed at the bottom of the specimen.

When analyzing the cutting geometry of the fiber laser, it was observed that the kerf geometry varies. It was observed that they widened towards both the top and bottom surfaces, and in some cases, the kerf even narrowed in the middle of the material [34]. However, another fiber-laser study [36] also found that the kerf narrowed towards the bottom surface. In this study, a 12 kW laser was used to cut a 25 mm thick plate of S235JR. Therefore, it can be assumed that when cutting thick materials with a fiber laser, the material to be cut absorbs a large amount of the energy applied to the cutting zone, which results in a different cut geometry than when cutting thinner materials. As a result, the taper of the kerf is determined not only by the parameters of the laser-cutting process but also by the type of laser used.

3.4. Results of the Laser Thermal-Effect Evaluation

The laser-cutting process is based on thermal energy output. Therefore, it is difficult to avoid high temperature exposure to the metal alloy during the cutting process. As a result of the aforementioned processes, a heat-affected zone (HAZ) is a phenomenon that is commonly identified in laser cutting. The material heats up during the process of laser cutting and then quickly cools down. As a consequence of this rapid cooling, changes in the crystal structure of the alloy are often observed; this is due to the remelting of material in the area of the workpiece that is affected by the temperature, in comparison with the uninfluenced part of the workpiece [7,37].

Therefore, six samples were selected for further laser thermal-effect analysis. The selection was based on the results of previous experiments on surface roughness, dimensional and geometric accuracy. Samples of both thicknesses were evaluated based on their respective values of these quality characteristics and were then compared to determine the overall best, medium and worst quality results. As a result, the selected samples were found to exhibit a range of cutting qualities, including good (4.03 and 6.02), medium (4.06 and 6.08) and poor (4.11 and 6.11).

The microstructure of low-carbon S355JR steel is composed of ferrite and pearlite grains due to the low carbon content of 0.23%. Analyzing the microstructure of the alloy after the laser-cutting process (Figure 14), it is obvious that the high temperature affected the microstructure of the area near the cut. Although there are no clear structural changes in the alloy, three zones are visible in the laser-affected area of the re-melted metal alloy: the heat-affected zone (HAZ), the transition zone, and the temperature-unaffected zone—the base material.

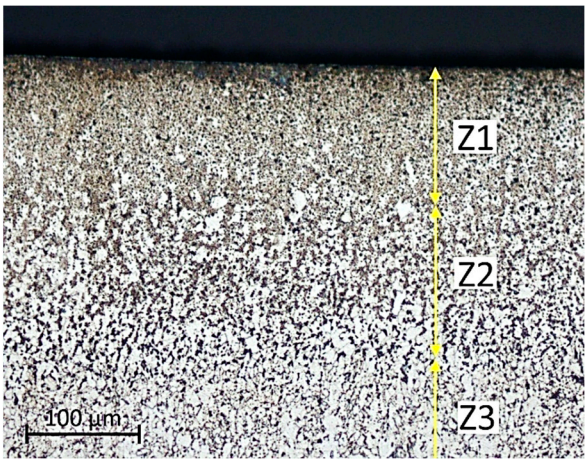

Figure 14. Temperature-affected zones of S355JR steel after laser cutting (6.08): Z1—HAZ; Z2—transition zone; Z3—base material.

Figure 15 shows microstructure images of the 4 mm thick samples. A narrow HAZ of approximately 33 µm thickness is visible. Ten HAZ measurements were taken for each evaluated sample, as shown in Figures 16–18.

As shown in Figure 19, the average HAZ depth of the 4 mm thick samples varies from 26.281 µm to 39.835 µm. Although sample 4.03 had good surface roughness and dimensional accuracy results, this sample has the highest average HAZ depth (39.835 µm). Therefore, it can be concluded that although the quality of the laser-cut part is relatively good, the depth of the heat-affected zone may be higher.

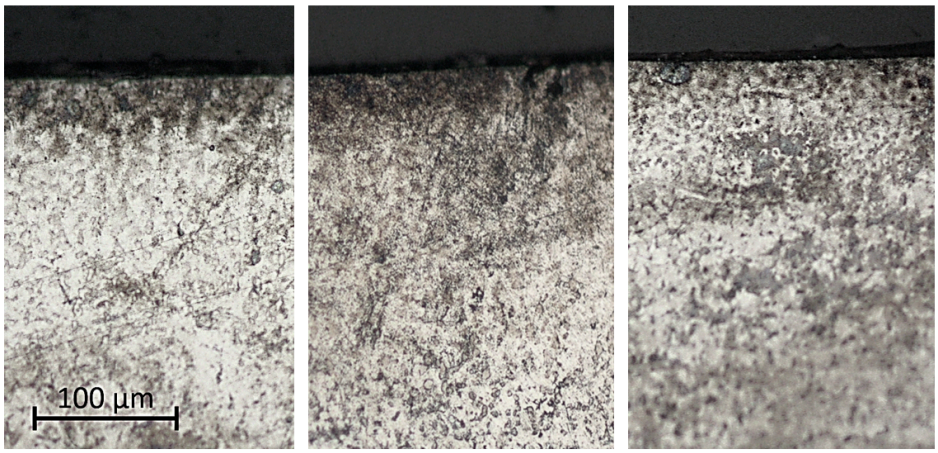

(**a**) (**b**) (**c**)

Figure 15. Microstructures of 4 mm thick samples: (**a**) 4.03; (**b**) 4.06; (**c**) 4.11.

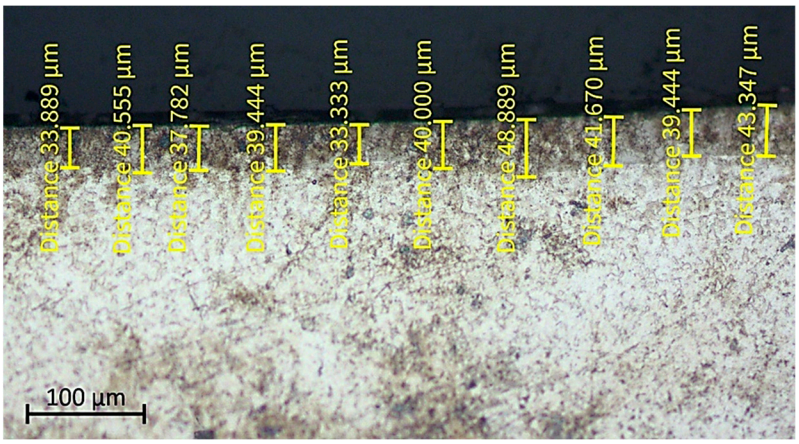

Figure 16. HAZ depth of the sample 4.03.

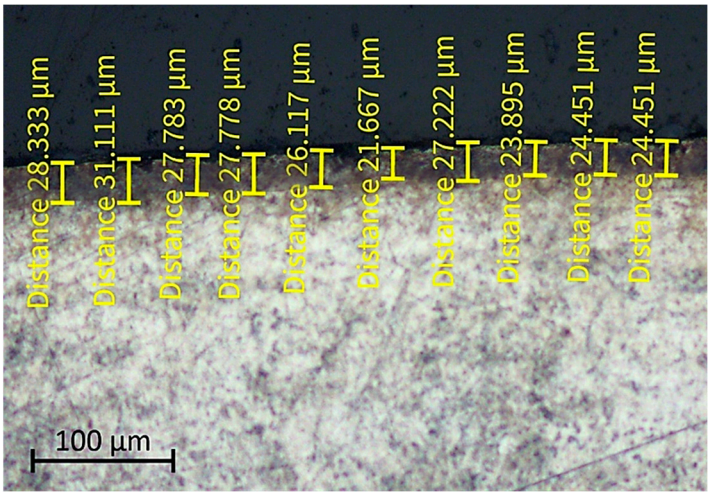

Figure 17. HAZ depth of the sample 4.06.

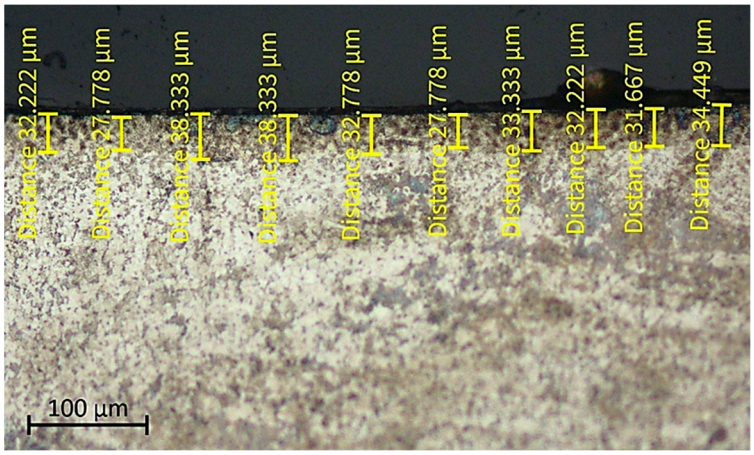

Figure 18. HAZ depth of the sample 4.11.

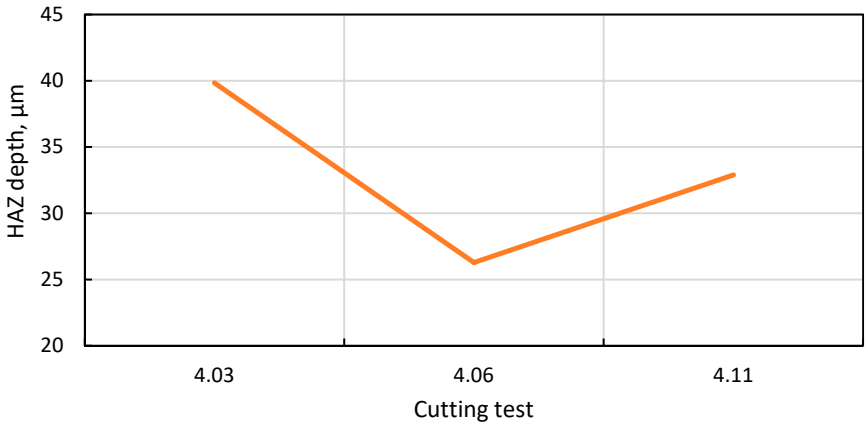

Figure 19. Variation of average HAZ depth of 4 mm thick samples.

When evaluating the influence of high temperature on the 6 mm thick samples, it is evident that the thermal effect on the microstructure (Figure 20) is significantly higher than on 4 mm thick samples. In this case, the average depth of the heat-affected zone of the specimens is 205.665 µm. It is also important to note that the cutting speed for properly cut 6 mm thick samples was lower than 4 mm. This means that the contact time between laser and material was also longer. As a result, the greater thickness of the material resulted in a deeper heat-affected zone during the laser-cutting process.

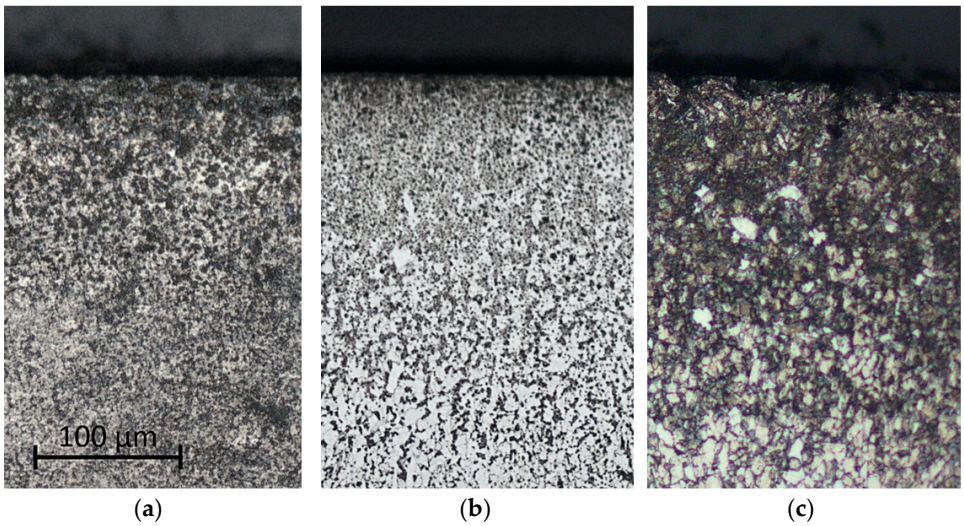

Figure 20. Microstructures of 6 mm thick samples: (**a**) 6.02; (**b**) 6.08; (**c**) 6.11.

It was found that the temperature-affected area of the 6 mm thick samples is smaller at the top of the laser cut. This is because the material melted on the top of the sample flows down, heating the bottom of the cut, where the thermal effect is larger. The HAZ depth values of the 6 mm thick samples are shown in Figures 21–23.

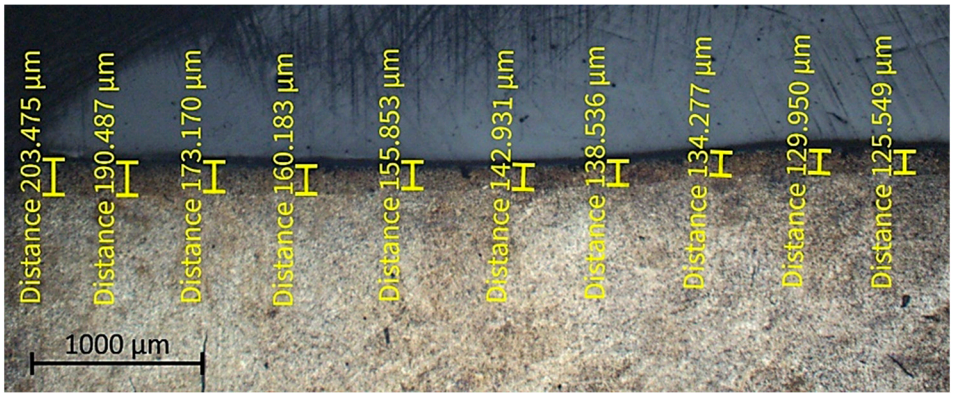

Figure 21. HAZ depth of the sample 6.02.

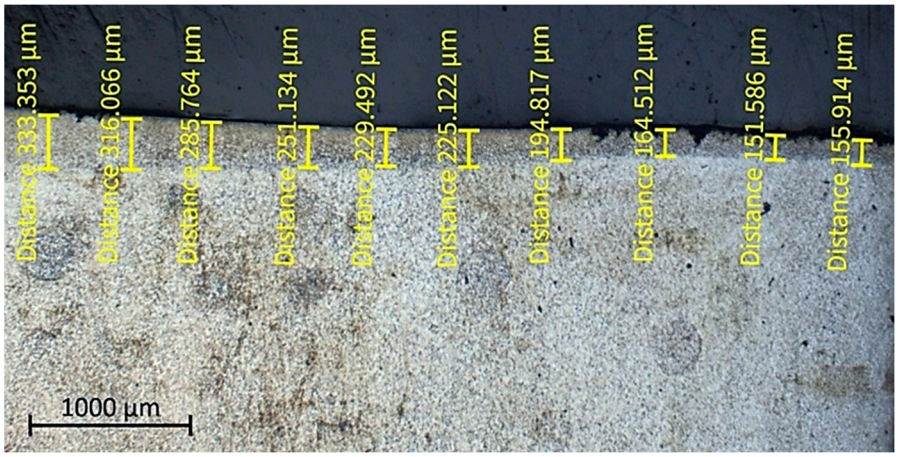

Figure 22. HAZ depth of the sample 6.08.

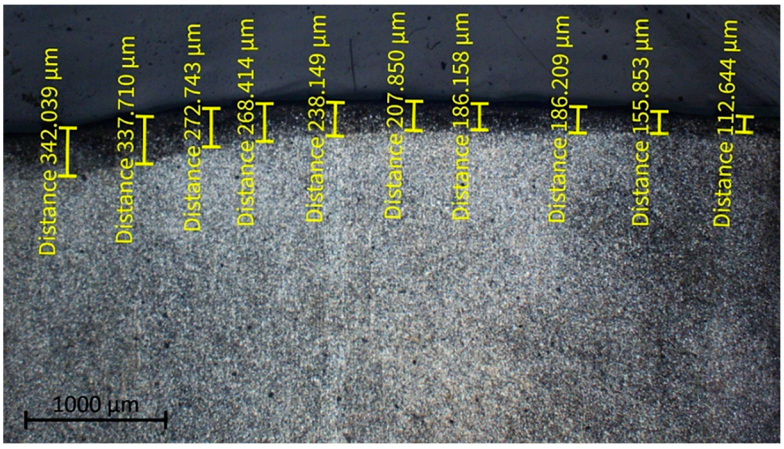

Figure 23. HAZ depth of the sample 6.11.

The heat-affected zone of the 6 mm thick samples ranges from 155.441 µm to 230.779 µm (Figure 24). The largest heat-affected zone was found in sample 6.11 (230.779 µm), which value is like sample 6.08 (230.776 µm). This sample also had the worst cut quality and accuracy of all the 4 and 6 mm thick samples.

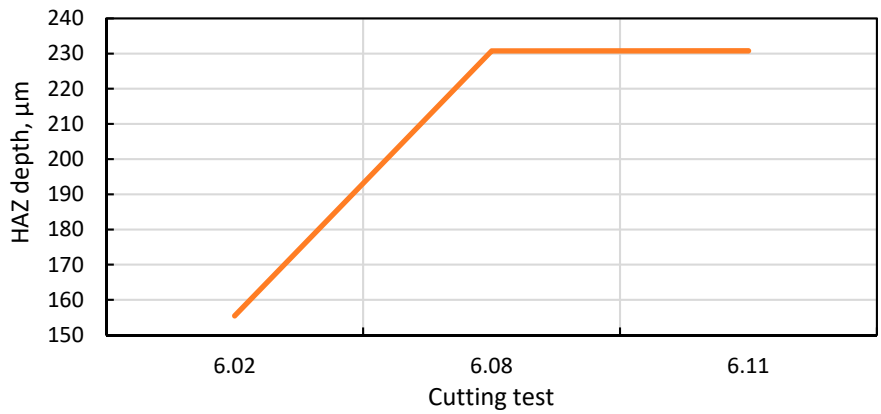

Figure 24. Variation of average HAZ depth of 6 mm thick samples.

Comparing the HAZ depth of the 4 mm and 6 mm samples, it is clear that the 4 mm thick metal plate was affected by a lower amount of heat during the laser-cutting process. This is due to the different linear energy applied to the cut area during laser cutting, as shown in Table 4. Specifically, the linear energy required to cut a 4 mm thick sample is lower than that required to machine a 6 mm thick material.

Table 4. HAZ depth with corresponding cutting parameters of the 4 and 6 mm thick samples.

Cutting Test	Laser Power, kW	Cutting Speed, mm/min	Auxiliary Gas Pressure, Bar	Linear Energy, J/mm	HAZ Depth, µm
4.03	3.2	3500	0.55	54.86	39.835
4.06	3.8	4000	0.55	57.00	26.281
4.11	3.8	3500	1.00	65.14	32.889
		Mean			33.002
6.02	3.5	2900	0.60	72.41	155.441
6.08	4.0	2400	0.60	100.00	230.776
6.11	4.0	2900	4.00	82.76	230.779
		Mean			205.665

The heat-affected zone depth values can be compared with other studies. In one study [37], the temperature effect of 8 mm thick S235JR steel was evaluated, and an average depth of heat-affected zone of 170 µm was determined. It is important to note that this study was performed using a CO_2 laser for cutting. This confirms that cutting thicker materials with a fiber laser has a greater temperature effect on the material than with a CO_2 laser. In another study [38], a 6 mm thick C45 steel plate was processed by varying the laser power and cutting speed. It was found that the HAZ is thicker when high laser power and a low cutting speed are used for cutting [38]. The same tendency is observed when comparing the cutting parameters of specimens 6.02 and 6.11. Both samples were cut at the same speed (v = 2900 mm/min), but increasing the power (P = 4 kW) resulted in a larger heat-affected zone in test 6.11.

3.5. Results of the Laser-Cutting Quality Optimization

The evaluation results of the laser-cutting quality characteristics were used to develop an artificial intelligence (AI)-based artificial neural network (ANN). The input parameters of the ANN were material thickness, laser power, cutting speed and auxiliary gas pressure. The output parameters were the obtained quality characteristics—average surface roughness Ra, average dimensional deviation, and kerf taper (Figure 25).

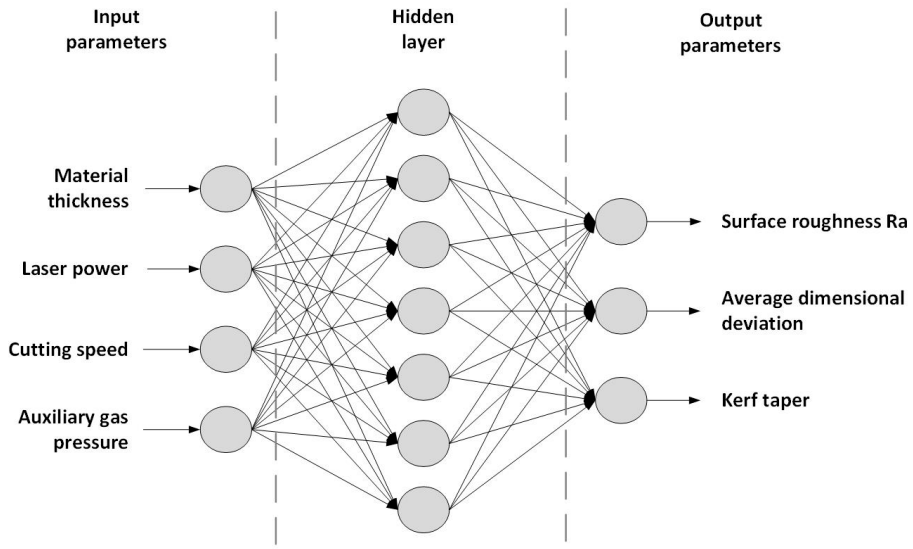

Figure 25. Structure of developed ANN.

The experimental data obtained from fifteen cut samples were used to train the ANN, and the remaining six data sets were used to test the developed neural network. To select the neural network with the best structure, training was performed with two to twenty neurons in the hidden layer. The mean squared error (MSE) between actual and predicted values was calculated for all tested ANN structures. Calculations showed that a hidden layer of seven neurons provides the most accurate prediction. Therefore, this ANN structure was used for further laser-cutting quality optimization. To achieve optimal laser-cutting quality, a minimization problem was solved. The aim was to ensure the lowest average surface roughness (*R*a), the lowest average dimensional deviation (ADD), and the lowest kerf taper (KT). The developed ANN has been used to predict the values of these quality characteristics for a set of the laser-cutting parameters that have not been tested during the cutting tests. The objective function *Z* is the sum of the estimated quality characteristics, which is calculated using Equation (5):

$$Z = Ra(t, P, v, p) + ADD(t, P, v, p) + KT(t, P, v, p), \quad (5)$$

where *Ra*—average surface roughness, µm; *ADD*—average dimensional deviation, mm; *KT*—kerf taper, mm; *t*—thickness of the material, mm; *P*—laser power, kW; *v*—cutting speed, mm/min; *p*—auxiliary gas pressure, bar. Based on the results of the cutting tests, the upper and lower limits of the cutting parameters for the optimization were determined according to material thickness:

$$\begin{aligned} &4\text{ mm—}2.8 \le P \le 4.0;\ 2900 \le v \le 4500; 0.30 \le p \le 4; \\ &6\text{ mm—}3.0 \le P \le 4.0;\ 2900 \le v \le 3500; 0.55 \le p \le 4. \end{aligned}$$

To determine the cutting parameters that would result in an optimal cut quality, optimization was performed for each thickness. The solution for 4 mm thickness was found after 32 iterations with an objective function value of 1.853. Similarly, for a thickness of 6 mm, the calculations were carried out 33 times until the best solution of the objective function was found with a value of 1.718. Table 5 shows the calculated optimum cutting parameters.

To assess the accuracy of the optimization using the obtained cutting parameters, the control samples 4.13 and 6.13 were cut and the quality characteristics were measured. The obtained results are presented in Table 6.

Table 5. Calculated optimal values of laser-cutting parameters.

Cutting Test	Laser Power, kW	Cutting Speed, mm/min	Auxiliary Gas Pressure, Bar	Iterations	Value of Objective Function
4.13	3.0	2900	0.40	32	1.853
6.13	3.9	3240	0.55	33	1.718

Table 6. Predicted and actual quality characteristics values of the cutting test 4.13 and 6.13 samples.

	Cutting Test	Predicted Value	Actual Value	Relative Error, %
Surface roughness *R*a, µm	4.13	1.344	1.609	−16.5
	6.13	1.432	1.930	−25.8
Dimensional deviation, mm	4.13	0.361	0.206	+75.2
	6.13	0.145	0.080	+81.3
Kerf taper, mm	4.13	0.148	0.195	−24.1
	6.13	0.141	0.103	+36.9

Comparing the actual values of the quality characteristics with the predicted values generated by the artificial neural network model, it can be observed that the actual values of the quality characteristics differ from the predicted values. The differences are minimal in the context of surface roughness and kerf taper measurements, but further training of the ANN could enhance dimensional deviation prediction.

Comparing the quality characteristics of control samples 4.13 and 6.13 with other samples, it is observed that the optimization was performed by increasing the roughness of the cut surface, seeking to achieve better dimensional accuracy and lower kerf taper. It is important to mention that ANNs are based on a learning process. The accuracy of the developed artificial neural network in predicting the values of quality characteristics and performing process optimization increases with the amount of data used for training the network. To improve the accuracy of the optimization model, the measured actual quality characteristics of samples 4.13 and 6.13 can be included in the data set used to train the network.

In conclusion, fiber-laser processing of thicker materials can be effectively improved using AI-based optimization models. An artificial neural network trained with research data on quality characteristics at different cutting parameters can quickly identify complex relationships between quality characteristics and cutting parameters, enabling more efficient process control.

4. Conclusions

In this paper, the effect of 4 kW fiber-laser cutting parameters (laser power, cutting speed and auxiliary gas pressure) on the surface roughness, cutting accuracy, kerf taper, and heat-affected zone depth on mild steel plates with thicknesses of 4 and 6 mm was experimentally investigated. The obtained results of cutting quality characteristics were used for process optimization. The major findings of this study are given below.

1. Surface roughness was found to be affected by all estimated laser-cutting parameters, including laser power, cutting speed, and auxiliary gas pressure. As the laser power increased from 2.8 kW to 4 kW, the average surface roughness (*R*a) reduced by 0.653 µm for 4 mm thick samples, and as the cutting speed increased from 2900 mm/min to 4500 mm/min, surface roughness decreased by 0.765 µm. The opposite trend was found when evaluating the influence of the auxiliary cutting gas pressure. As the pressure increased from 0.3 bar to 1.5 bar, the cut surface roughness also increased from 1.264 µm to 2.979 µm. The same influence of cutting parameters on the roughness of the cut surface was found by analyzing the surface roughness results of the 6 mm thick samples. However, comparing the samples of different thicknesses cut

with similar parameters, it was found that the surface roughness of the 6 mm thick sample is 0.237 μm lower.

2. The lowest average dimensional deviation when cutting a 4 mm thick steel plate was found to be 0.225 mm and 0.096 mm for a 6 mm thick steel plate. Therefore, the accuracy is significantly influenced by the thickness of the material. The thicker the material, the smaller the deviation from the nominal dimensional values observed. Also, the cutting accuracy is mostly affected by the laser power. As the laser power increased from 2.8 kW to 4 kW, the average dimensional deviation of 4 mm thick specimens increased by 0.086 mm and 6 mm thick specimens increased by 0.059 mm (as the power increased from 3 kW to 4 kW). Otherwise, cutting speed and auxiliary gas pressure did not have a significant impact on the cutting accuracy.
3. According to the result of the kerf taper evaluation, the laser-cut kerf widens toward the bottom of the cut. In addition, as the material thickness increases, the kerf taper also increases from 0.056 mm (at 4 mm thickness) to 0.199 mm (at 6 mm thickness). Also, laser power and cutting speed have a major impact on the kerf taper for both thicknesses. For instance, when cutting a 4 mm thick plate, as the laser power increased from 2.8 kW to 4 kW, the kerf taper decreased from 0.074 mm to 0.041 mm. However, it increased from 0.027 mm to 0.104 mm as the cutting speed was increased (from 2900 mm/min to 4500 mm/min). The influence of the auxiliary gas pressure on the kerf taper is not significant until the auxiliary gas pressure is high. For example, at a gas pressure of 4 bar, the kerf taper of the 6 mm thick sample increased to 0.337 mm.
4. The depth of the heat-affected zone increases toward the bottom of the sample and depends on the thickness of the material. For instance, the HAZ depth of 4 mm thick samples varies from 26.281 μm to 39.835 μm. In contrast, the thermal effect on 6 mm thick samples is about six times larger—the depth of the heat-affected zone varies from 155.441 μm to 230.779 μm.
5. Optimal cutting parameters were calculated using a developed AI-based optimization model for laser-cutting quality. As a result, it is recommended to use a laser power of 3 kW, a cutting speed of 2900 mm/min, and an auxiliary oxygen gas pressure of 0.4 bar to cut a 4 mm thick plate. In addition, it was also found that the optimal cutting quality for a 6 mm thick plate will be obtained when the laser power is 3.9 kW, the cutting speed is 3240 mm/min, and the auxiliary gas pressure is 0.55 bar.
6. The achieved results encouraged the authors to continue research related to the study of real situations in the field of industrial production, as this brings obvious benefits to the quality of the manufactured products. Further research will expand into the examination of the morphology of the cut surface, as defect cracks were observed on the cut surface during this study. The last study only provided data for one commonly used material; in the future, more materials used in industry could be included to provide more recommendations. Collecting more experimental data will allow for a more accurate determination of optimal cutting parameters using ANNs.

Author Contributions: Conceptualization, R.B.; methodology, L.C.; software, L.C.; validation, L.C.; formal analysis, R.B.; investigation, L.C.; resources, L.C.; data curation, L.C.; writing—original draft preparation, L.C.; writing—review and editing, R.B.; visualization, L.C.; supervision, R.B. All authors have read and agreed to the published version of the manuscript.

Funding: This research received no external funding.

Data Availability Statement: The original contributions presented in the study are included in the article, further inquiries can be directed to the corresponding author.

Conflicts of Interest: The authors declare no conflicts of interest.

References

1. Gamage, J.R.; DeSilva, A.K.M. Assessment of Research Needs for Sustainability of Unconventional Machining Processes. *Procedia CIRP* **2015**, *26*, 385–390. [CrossRef]
2. Reiff, C.; Buser, M.; Betten, T.; Onuseit, V.; Hossfeld, M.; Wehner, D.; Riedel, O. A Process-Planning Framework for Sustainable Manufacturing. *Energies* **2021**, *14*, 5811. [CrossRef]
3. Öztürk, E.G.; Ayturan, Z.C. Life Cycle Impact Assessment And Economic Evaluation of Material Cutting Technologies. In Proceedings of the 5th International Conference on Energy and Environment: Bringing Together Engineering and Economics, Porto, Portugal, 2–3 June 2022.
4. Kellens, K.; Rodrigues, G.C.; Dewulf, W.; Duflou, J. Energy and Resource Efficiency of Laser Cutting Processes. *Phys. Procedia* **2014**, *56*, 854–864. [CrossRef]
5. Alwis, A.M.L.D.; Silva, N.D.; Samaranayake, P. Industry 4.0-Enabled Sustainable Manufacturing: Current Practices, Barriers and Strategies. *Benchmarking Int. J.* 2023, *ahead-of-print*. [CrossRef]
6. Gupta, K.; Gupta, M.K. Developments in Nonconventional Machining for Sustainable Production: A State-of-the-Art Review. *Proc. Inst. Mech. Eng. Part C J. Mech. Eng. Sci.* **2019**, *233*, 4213–4232. [CrossRef]
7. Liao, Z.; la Monaca, A.; Murray, J.; Speidel, A.; Ushmaev, D.; Clare, A.; Axinte, D.; M'Saoubi, R. Surface Integrity in Metal Machining—Part I: Fundamentals of Surface Characteristics and Formation Mechanisms. *Int. J. Mach. Tools Manuf.* **2021**, *162*, 103687. [CrossRef]
8. Ullah, S.; Li, X.; Guo, G.; Rodríguez, A.R.; Li, D.; Du, J.; Cui, L.; Wei, L.; Liu, X. Influence of the Fiber Laser Cutting Parameters on the Mechanical Properties and Cut−edge Microfeatures of a AA2B06−T4 Aluminum Alloy. *Opt. Laser Technol.* **2022**, *156*, 108395. [CrossRef]
9. Santolini, G.; Rota, P.; Gandolfi, D.; Bosetti, P. Cut Quality Estimation in Industrial Laser Cutting Machines: A Machine Learning Approach. In Proceedings of the 2019 IEEE/CVF Conference on Computer Vision and Pattern Recognition Workshops (CVPRW 2019), Long Beach, CA, USA, 16–17 June 2019; pp. 389–397. [CrossRef]
10. Youssef, H.; El-Hofy, H. *Non-Traditional and Advanced Machining Technologies*; Routledge: London, UK, 2020; ISBN 978-1-00-305531-0.
11. la Monaca, A.; Murray, J.W.; Liao, Z.; Speidel, A.; Robles-Linares, J.A.; Axinte, D.A.; Hardy, M.C.; Clare, A.T. Surface Integrity in Metal Machining—Part II: Functional Performance. *Int. J. Mach. Tools Manuf.* **2021**, *164*, 103718. [CrossRef]
12. Krajewski, S.J.; Grochala, D.; Tomkow, J.; Grzejda, R. Analysis of the Surface Stereometry of Alloyed Austenitic Steel after Fibre Laser Cutting Using Confocal Microscopy. *Coatings* **2023**, *13*, 15. [CrossRef]
13. Sureban, R.; Kulkarni, V.N.; Gaitonde, V.N. Modem Optimization Techniques for Advanced Machining Processes—A Review. *Mater. Today Proc.* **2019**, *18*, 3034–3042. [CrossRef]
14. Zlamal, T.; Malotova, Š.; Petru, J.; Brytan, Z.; Musil, V. The Evaluation of the Surface Quality after Laser Cutting. *MATEC Web Conf.* **2018**, *244*, 02009. [CrossRef]
15. Amaral, I.; Silva, F.J.G.; Pinto, G.F.L.; Campilho, R.D.S.G.; Gouveia, R.M. Improving the Cut Surface Quality by Optimizing Parameters in the Fibre Laser Cutting Process. *Procedia Manuf.* **2019**, *38*, 1111–1120. [CrossRef]
16. Bakhtiyari, A.N.; Wang, Z.; Wang, L.; Zheng, H. A Review on Applications of Artificial Intelligence in Modeling and Optimization of Laser Beam Machining. *Opt. Laser Technol.* **2021**, *135*, 106721. [CrossRef]
17. Vagheesan, S.; Govindarajalu, J. Hybrid Neural Network-Particle Swarm Optimization Algorithm and Neural Network-Genetic Algorithm for the Optimization of Quality Characteristics during CO_2 Laser Cutting of Aluminium Alloy. *J. Braz. Soc. Mech. Sci. Eng.* **2019**, *41*, 328. [CrossRef]
18. Yongbin, Y.; Bagherzadeh, S.A.; Azimy, H.; Akbari, M.; Karimipour, A. Comparison of the Artificial Neural Network Model Prediction and the Experimental Results for Cutting Region Temperature and Surface Roughness in Laser Cutting of AL6061T6 Alloy. *Infrared Phys. Technol.* **2020**, *108*, 103364. [CrossRef]
19. Javaid, M.; Haleem, A.; Singh, R.P.; Khan, S.; Suman, R. Sustainability 4.0 and Its Applications in the Field of Manufacturing. *Internet Things Cyber Phys. Syst.* **2022**, *2*, 82–90. [CrossRef]
20. Awan, U.; Sroufe, R.; Shahbaz, M. Industry 4.0 and the Circular Economy: A Literature Review and Recommendations for Future Research. *Bus. Strategy Environ.* **2021**, *30*, 2038–2060. [CrossRef]
21. Balamurugan, E.; Flaih, L.R.; Yuvaraj, D.; Sangeetha, K.; Jayanthiladevi, A.; Kumar, T.S. Use Case of Artificial Intelligence in Machine Learning Manufacturing 4.0. In Proceedings of the 2019 International Conference on Computational Intelligence and Knowledge Economy (Iccike' 2019), Dubai, United Arab Emirates, 11–12 December 2019; pp. 657–660. [CrossRef]
22. Kalita, K.; Chakraborty, S.; Ghadai, R.K.; Chakraborty, S. Parametric Optimization of Non-Traditional Machining Processes Using Multi-Criteria Decision Making Techniques: Literature Review and Future Directions. *Multiscale Multidiscip. Model. Exp. Des.* **2023**, *6*, 1–40. [CrossRef]
23. Sołtysiak, R.; Wasilewski, P.; Sołtysiak, A.; Troszyński, A.; Maćkowiak, P. The Analysis of Fiber and CO_2 Laser Cutting Accuracy. *MATEC Web Conf.* **2019**, *290*, 03016. [CrossRef]
24. Riveiro, A.; Quintero, F.; Boutinguiza, M.; del Val, J.; Comesana, R.; Lusquinos, F.; Pou, J. Laser Cutting: A Review on the Influence of Assist Gas. *Materials* **2019**, *12*, 157. [CrossRef]
25. Bohdal, L.; Schmidtke, D. Effect of Fiber and CO_2 Lasers Parameters on the Cut Surface Quality of RVS 1.4301 Stainless Steel. *J. Mech. Eng. Sci.* **2022**, *16*, 8862–8872. [CrossRef]

26. Madic, M.; Radovanovic, M.; Manic, M.; Trajanovic, M. Optimization of ANN Models Using Different Optimization Methods for Improving CO_2 Laser Cut Quality Characteristics. *J. Braz. Soc. Mech. Sci. Eng.* **2014**, *36*, 91–99. [CrossRef]
27. Fischer, U.; Gomeringer, R.; Heinzler, M.; Kilgus, R.; Näher, F.; Oesterle, S.; Paetzold, H.; Stephan, A. *Mechanical Engineer's Handbook*; Lithuanian Engineering Industry Association LINPRA: Vilnius, Lithuania, 2014; ISBN 978-609-02-1076-5.
28. Velling, A. Structural Steels S235, S275, S355, S420 and Their Properties. Available online: https://www.fractory.com/structural-steels-s235-s275-s355-s420-and-their-properties/ (accessed on 24 September 2023).
29. Girdu, C.C.; Mihail, L.A.; Dragoi, M.V. Estimation of Laser Cutting Process Efficiency. *IOP Conf. Ser. Mater. Sci. Eng.* **2019**, *659*, 012045. [CrossRef]
30. *ISO 4287:1997*; Geometrical Product Specifications (GPS)—Surface Texture: Profile Method—Terms, Definitions and Surface Texture Parameters. International Organization for Standardization: Geneva, Switzerland, 1997.
31. *ISO 9013:2017*; Thermal Cutting—Classification of Thermal Cuts—Geometrical Product Specification and Quality Tolerances. International Organization for Standardization: Geneva, Switzerland, 2017.
32. Madic, M.; Marinkovic, V.; Radovanovic, M. Optimization of the Kerf Quality Characteristics in CO_2 Laser Cutting of AISI 304 Stainless Steel Based on Taguchi Method. *Mechanika* **2013**, *19*, 580–587. [CrossRef]
33. Naresh; Khatak, P. Laser Cutting Technique: A Literature Review. *Mater. Today Proc.* **2022**, *56*, 2484–2489. [CrossRef]
34. Stelzer, S.; Mahrle, A.; Wetzig, A.; Beyer, E. Experimental Investigations on Fusion Cutting Stainless Steel with Fiber and CO_2 Laser Beams. *Phys. Procedia* **2013**, *41*, 399–404. [CrossRef]
35. Genna, S.; Menna, E.; Rubino, G.; Tagliaferri, V. Experimental Investigation of Industrial Laser Cutting: The Effect of the Material Selection and the Process Parameters on the Kerf Quality. *Appl. Sci.* **2020**, *10*, 4956. [CrossRef]
36. Liu, Y.; Zhang, S.; Zhao, Y.; Ren, Z. Experiments on the Kerf Quality Characteristic of Mild Steel While Cutting with a High-Power Fiber Laser. *Opt. Laser Technol.* **2022**, *154*, 108332. [CrossRef]
37. Saternus, Z.; Kubiak, M.; Piekarska, W.; Domanski, T. Analysis of Hardening Area of Material with Variable Parameters of Laser Beam Cutting. *Acta Phys. Pol. A* **2022**, *142*, 97–100. [CrossRef]
38. Boujelbene, M.; Alghamdi, A.; Miraoui, I.; Bayraktar, E.; Gazbar, M. Effects of the Laser Cutting Parameters on the Micro-Hardness and on the Heat Affected Zone of the Mi-Hardened Steel. *Int. J. Adv. Appl. Sci.* **2017**, *4*, 19–25. [CrossRef]

Disclaimer/Publisher's Note: The statements, opinions and data contained in all publications are solely those of the individual author(s) and contributor(s) and not of MDPI and/or the editor(s). MDPI and/or the editor(s) disclaim responsibility for any injury to people or property resulting from any ideas, methods, instructions or products referred to in the content.